The Impact of Measurement Biases on Availability for CAT III LAAS

Jason Rife and Sam Pullen, *Stanford University*

ABSTRACT

The original error description for the Local Area Augmentation System (LAAS) assumed unbiased measurement errors. In practice, however, satellite ranging errors may exhibit nonzero means. The LAAS error bound must account for these biases. This requirement places a particularly stringent demand on Category III (CAT III) LAAS, a future LAAS variant that will enable safe automated landing through rollout.

This paper examines the availability impact of biases on CAT III LAAS. To provide an upper limit for tolerable LAAS biases, the paper first considers an improved LAAS messaging structure and asks, for this ideal case, what maximum level of bias is tolerable. Even in the ideal case, the maximum bias at worst-case CONUS airports is only 4-8 cm. This baseline case assumes a nominal LAAS error distribution and a relaxed Vertical Alert Limit (VAL) of 10 m. To tolerate larger biases, improvements to the nominal LAAS are required. For instance, a dual-frequency LAAS implementation can tolerate biases as high as 14-30 cm, even with a tighter VAL of 5.3 m.

Tolerable biases for nonideal bounding algorithms are also considered. In order to achieve ideal performance, the LAAS message must be changed to transmit bias parameters to the airborne user. Preferably, the bias-protection algorithm would not require modification of the existing LAAS specification. Sigma inflation methods represent an alternative to bias-parameter transmission that requires no LAAS specification change but, consequently, that delivers somewhat lower bias tolerance. Performance varies widely for different classes of sigma inflation. Simulations indicate that the best-performing sigma inflation method (real-time position-domain inflation) nearly matches the bias tolerance possible with bias-parameter transmission. Unlike bias-parameter transmission, however, the bias tolerance for sigma-inflation methods depends strongly on possessing precise knowledge of the airborne error, σ_{air}, at the LAAS ground facility (LGF).

INTRODUCTION

In order to guarantee integrity, a Local Area Augmentation System (LAAS) must provide a confidence bound for its differential GPS corrections. Early LAAS concepts have relied on confidence bounds based on the assumption of zero-mean error distributions for each ranging source. In fact, experience with prototype hardware has demonstrated that LAAS differential corrections may exhibit small, nonzero biases. Because these biases may vary in time, they are difficult to estimate and subtract from differential GPS corrections. Consequently, the LAAS confidence bound should include terms to protect not only for random errors but also for these systematic biases.

Biases result from three principal mechanisms: calibration error, signal-in-space error, and the folding of distribution anomalies into the position solution. The first classification, the calibration bias, reflects the difficulties of characterizing antenna and receiver hardware. A single calibration curve may be insufficient to describe antenna phase center, for instance, because of variations among units from the same batch and because of temporal changes caused by environment exposure. The second classification, the signal-in-space bias, describes distortions to the incoming GPS waveform, such as those caused by spectral multipath. Multipath events introduce a site-specific bias that repeats each sidereal day. Finally, the third classification, the anomaly convolution bias, occurs when ranging error-distribution anomalies, such as asymmetries or secondary peaks, are converted into the position domain. This phenomenon is described in detail by [1].

Biases have particular significance for Category III (CAT III), an advanced version of LAAS which will enable a full autoland capability for aircraft on approach. Given the demanding safety requirements for autoland, CAT III LAAS offers little margin to tolerate biases. Even a small increase in the magnitude of the LAAS integrity bound, called the Protection Level (PL), may cause the PL to exceed an alert limit (AL) and thereby to trigger

temporary system unavailability. The rigid structure of the existing LAAS message aggravates this unavailability by causing PL inflation to be unnecessarily conservative.

This paper relaxes the LAAS message format to determine the maximum bias level that can be tolerated for CAT III. Although altering the LAAS message entails a potentially expensive specification change, the transmission of new measurement-bias parameters to the airborne user would enable formation of the tightest possible error bound. The specific modifications required to implement this high performance approach would impact both the Interface Control Document [2], to permit transmission of new parameters, and also the Minimum Operational Performance Standards [3], to implement a modified PL in the airborne receiver. At least as a theoretical exercise, analysis of bias-parameter transmission offers a means to define an upper bound on tolerable measurement biases.

An alternative approach to bias protection that sacrifices performance to avoid a specification change is sigma inflation. Sigma-inflation scales existing broadcast parameters to guarantee that the user PL is at least as large as the "ideal" PL. Several sigma-inflation methods are considered in this paper including sigma-relative inflation, excess-mass inflation, offline position-domain inflation and real-time position-domain inflation. Availability simulation permits the comparison of these sigma-inflation methods to the more aggressive approach of bias-parameter transmission.

The paper begins by developing a tight PL bound that retains integrity when ranging measurements are biased. Subsequent sections introduce models for the systematic bias and random error used in defining this tight PL. The ensuing section describes means of implementing the desired PL, both exactly, through bias-parameter transmission, and approximately, through conservative methods for sigma-inflation. Next, the paper describes a tool for availability simulation, which enables performance characterization of these different bias-protection strategies. Based on simulation results, the final section examines the maximum tolerable bias level achieved with bias-parameter transmission and the comparative performance possible with sigma-inflation.

VERTICAL PROTECTION LEVEL (VPL) WITH BIASED PSEUDORANGE CORRECTIONS

This section develops a LAAS error bound expression that protects for both random errors and systematic biases. The particular error bound described in this section is a Vertical Protection Level (VPL). The focus on the vertical reflects the tighter demands for vertical navigation, since vertical errors represent a more significant hazard than horizontal errors during landing and since satellite geometry provides poorer position resolution in the vertical direction.

The VPL expression that protects for measurement biases, $\mathrm{VPL}_{\mathrm{bias}}$, is a modified version of the nominal VPL expression, $\mathrm{VPL}_{\mathrm{nom}}$, which is given by the LAAS specifications. In fact, the LAAS specifications include multiple $\mathrm{VPL}_{\mathrm{nom}}$ expressions for different fault hypotheses; because the fault-free, or H0, hypothesis generally dominates the other VPL expressions, only the H0 case will be considered in this paper. For the H0 case, the $\mathrm{VPL}_{\mathrm{nom}}$ expression is simply an error bound based on the assumption of independent, unbiased Gaussian errors for each satellite ranging source. The probability of an outlier falling beyond the confidence bound is embedded in the scaling factor, K_{ffmd}. The satellite geometry and accuracy are embedded in the weighting coefficients, $S_{v,i}$, for each satellite, i.

$$VPL_{\mathrm{nom}} = VPL_{\mathrm{H0}} = K_{ffmd}\sqrt{\sum_{i=1}^{N} S_{v,i}^2 \sigma_i^2} \qquad (1)$$

The standard deviation for each ranging source is σ_i. This sigma term combines independent errors for each ranging measurement, including ground receiver noise, airborne receiver noise, nominal ionosphere gradients, and nominal troposphere gradients.

$$\sigma_i^2 = \sigma_{gnd,i}^2 + \sigma_{air,i}^2 + \sigma_{iono,i}^2 + \sigma_{tropo,i}^2 \qquad (2)$$

If ranging errors are biased by an unknown, but bounded, systematic offset, then the nominal VPL expression no longer guarantees system integrity. Assuming that the unknown bias on each ranging source is bounded by a term μ_i, then the total positioning error associated with all biases is bounded by μ_p.

$$\mu_p = \sum_{i=1}^{N} \left| S_{v,i} \mu_i \right| \qquad (3)$$

A conservative expression that provides integrity for both random Gaussian errors and systematic biases can be obtained by adding expressions (1) and (3). This conservative protection level expression is labeled $\mathrm{VPL}_{\mathrm{bias}}$.

$$VPL_{bias} = K_{ffmd}\sqrt{\sum_{i=1}^{N} S_{v,i}^2 \sigma_i^2} + \sum_{i=1}^{N} \left| S_{v,i} \mu_i \right| \qquad (4)$$

Implementing $\mathrm{VPL}_{\mathrm{bias}}$ in an operational system would require a significant change to the existing LAAS specifications. In the LAAS system, the VPL expression

is evaluated at the aircraft and compared to the Vertical Alert Limit (VAL), a category-specific parameter defining the boundary for hazardously large errors. In order for the aircraft to evaluate the VPL_{bias} expression, however, the LAAS ground facility would need to transmit the satellite-specific bias parameters, μ_i, to the aircraft. Further revisions to the airborne equipment would be required to add the bias term, (3), to the existing nominal VPL expressions.

This paper seeks, first, to establish a limit on tolerable biases using the "ideal" VPL_{bias} expression defined in this section and, second, to compare this upper limit to the performance for alternative bias-protection strategies, which avoid specification changes by conservatively approximating VPL_{bias}. In order to assess the maximum tolerable bias, it is first necessary to introduce error models that bound the systematic biases, μ_i, and the random error sigmas, σ_i, associated with each ranging measurement, i,.

COMPARISON OF BIAS MODELS

This section focuses on establishing a theoretical bound for the systematic ranging bias. Since the specific form of this bias bound will depend strongly on the hardware fielded for the LAAS system, several alternative structures for the bias bound are described. Altogether, three models are considered: an absolute-bias model, a sigma-relative model, and a piecewise-linear model. The three models are illustrated together in Figure 1. These models, each normalized by a maximum bias, μ_{max}, describe the bias-bound magnitude as a function of satellite elevation. In availability simulations, the largest tolerable bias can be determined by adjusting the parameter μ_{max} upward until system availability drops to an unacceptable level.

Absolute Bias Model

This simple model treats all biases as uniform, at an absolute level expressed in meters. This model has been previously discussed by several authors including DeCleene [4], van Graas [5], and Rife [1]. An expression for the absolute-bias bound is

$$\mu_i(E_i)/\mu_{max} = 1. \qquad (5)$$

Sigma-Relative Bias Model

In some cases, especially with strong specular multipath, systematic biases may be large at low elevations, where the random error is also large. For such cases, a reasonable bound for the systematic bias is proportional to the standard deviation, σ_i. This model has been invoked in several previous studies, including [4], [6] and [7]. As defined here, the maximum relative-sigma bias is defined at a reference elevation, E_{ref}.

$$\frac{\mu_i(E_i)}{\mu_{max}} = \frac{\sigma_i(E_i)}{\sigma_i(E_{ref})}, \quad E_i \geq E_{ref} \qquad (6)$$

Since the μ_{max} parameter increases dramatically as E_{ref} approaches zero, a nonzero reference angle (of 1°) was selected for this paper, to assist in comparison of the maximum tolerable bias among the various bias models. In practice, it is unnecessary to define the model below E_{ref}, since these satellites are not approved by LAAS.

Piecewise-Linear Bias Model

In an actual system the peak bias may not occur at the lowest elevation angle. To simulate generalized bias functions, a piecewise-linear model is useful. As an example of a bias function that does not follow either the absolute or sigma-relative models, Figure 1(b) illustrates bias data for a Multipath Limiting Antenna (MLA) as measured by the William J. Hughes Federal Aviation Administration (FAA) Technical Center. For this data, the largest bias level occurs at approximately a 30° elevation angle. A piecewise model that bounds the FAATC data is

$$\frac{\mu_i(E_i)}{\mu_{max}} = \begin{cases} \left(\frac{2}{3} + \frac{2}{3}\frac{(E_i - 5°)}{25°}\right) & E_i \leq 30° \\ \left(1 - \frac{2}{3}\frac{(E_i - 30°)}{10°}\right) & 30° < E_i \leq 40° \\ \frac{1}{3} & 40° < E_i \end{cases}. \qquad (7)$$

For the FAATC data presented in Figure 1(b), the bounding μ_{max} parameter for the piecewise (and absolute) models is 7.5 cm. For the relative bound, it is 19.0 cm.

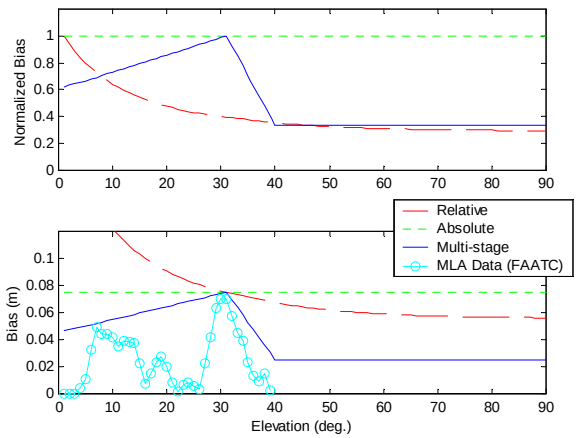

Figure 1. Bias Model Comparison

COMPARISON OF SIGMA MODELS

A model of the random error parameter, σ_i, is also necessary to simulate VPL_{bias}. The standard sigma model for LAAS was proposed by McGraw *et al.* [8]. This baseline model captures the nominal noise performance expected for a ground station with a multipath-limiting antenna. For CAT III operations, however, the availability achieved using this baseline error model, even in the unbiased case, is significantly lower than desired. As a consequence, other researchers have proposed both tighter error bounds and alternative hardware configurations, as summarized by Shively [9].

This paper considers two alternative error models in addition to the nominal model. The first is a reduced airborne error model, that attempts to remove excess conservatism from the Airborne Accuracy Designator (AAD) curve. The second is a dual-frequency error model, which benefits from additional smoothing which will be possible using divergence-free corrections based on L1 and L5 measurements.

Nominal Error Model

The nominal sigma model treats LAAS ranging errors as independent Gaussian distributions with standard deviation σ_i. This sigma term is the root-sum-square of errors associated with the ground receiver, with the airborne receiver, and with ionosphere and troposphere gradients, as described by (2). The nominal sigmas for each of these terms are defined as follows.

Assuming four MLAs at the ground station, the ground contribution to the random error can be characterized by the Ground Accuracy Designator (GAD) "C4" curve [8].

$$\sigma_{gnd,i}(E_i) = \sqrt{\tfrac{1}{4}(\sigma_{RR})^2 + 0.04^2 + \left(\frac{0.01}{\sin(E_i)}\right)^2}$$
$$\sigma_{RR,i} = \begin{cases} 0.15 + 0.84e^{-E_i/15.5^\circ} & E_i \le 35^\circ \\ 0.24 & 35^\circ < E_i \end{cases} \quad (8)$$

The corresponding sigma for the airborne receiver is described by the Aircraft Accuracy Designator (AAD) curves. In particular, the "B" curve (AAD-B) should bound the random error for CAT III-qualified airborne equipment.

$$\sigma_{air,i}(E_i) = \sqrt{\sigma^2_{air\_noise,i} + \sigma^2_{air\_multipath,i}}$$
$$\sigma_{air\_noise,i} = 0.11 + 0.13e^{-E_i/4^\circ} \quad (9)$$
$$\sigma_{air\_multipath,i} = 0.13 + 0.53e^{-E_i/10^\circ}$$

The ionosphere sigma model consists of two parts, a first term associated with the differential delay caused by random ionospheric gradients and a second term associated with carrier-smoothing divergence. In defining these two terms, a number of parameters are employed, including the obliquity factor, *OF*, the vertical ionosphere gradient standard deviation, σ_{vig} (taken as 4 mm/km), the distance between the aircraft and the ground facility antenna centroid, X (taken as 6 km), the filter smoothing time, τ (taken as 100 s), and the aircraft approach velocity, V_{air} (bounded by 0.13 km/s).

$$\sigma_{iono\_red,i}(E_i) = OF(E_i) \cdot \sigma_{vig}(X + 2\tau V_{air}) \quad (10)$$

The troposphere error is assumed much smaller than the other error sources, and is neglected for this analysis.

$$\sigma_{trop,i} = 0 \quad (11)$$

Figure 2 illustrates the total error, as a function of elevation, which results from combining all four error sources.

In availability simulations, this nominal error model results in large VPL values and unacceptable availability if the VAL is set to the specified CAT III level of 5.3 m. The precise level of the VAL parameter for CAT III remains under discussion, however, and may eventually increase as high as 10 m. For a 10 m VAL, the nominal error distribution delivers an acceptable availability (>0.999), as discussed by Shively [9].

Reduced Airborne

Alternatives to the nominal error model can achieve acceptable availability for a lower VAL. A reduced airborne model, for instance, shrinks the total error curve by removing excess conservatism associated with σ_{air}. This reduced airborne model is described by the LAAS Minimum Aviation System Performance Standards

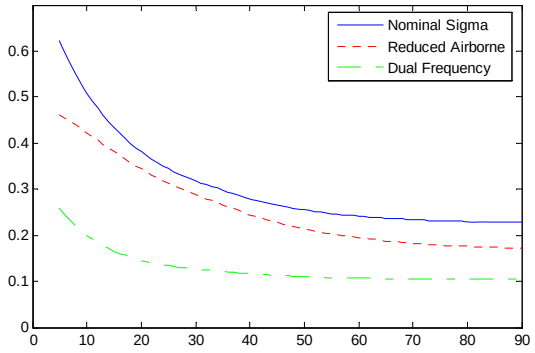

Figure 2. Sigma Models for Random Error

(MASPS) [10] and provides a shaper airborne bound than (9), more in line with data measured from actual airborne receivers. The reduced airborne noise model is

$$\sigma_{air,i}\left(E_i\right) = 0.074 + 0.18e^{-E_i/27.7^\circ} . \quad (12)$$

The reduced airborne model treats all other error terms as equivalent to those of the nominal model. The total error for the reduced airborne model is, nonetheless, significantly smaller than the nominal total error, as shown in Figure 2. A consequence of this smaller total sigma is that the model achieves an acceptable availability if VAL is 9 m or larger [9].

Dual Frequency

A future dual-frequency capability, based on L5, would enable further reduction of the total error curve. In fact, availability simulations suggest that a dual-frequency LAAS could achieve acceptable availability for a VAL as low as 5.3 m, the level currently specified for CAT III LAAS [9].

Of the many methods for combining dual-frequency measurements, McGraw recommends divergence-free smoothing [11]. The raw noise level for divergence-free smoothing is similar to that for single-frequency carrier smoothing. In an ionosphere gradient, however, the divergence-free solution accumulates no code-carrier divergence error. Thus the ionosphere error depends only on the differential gradient between the ground station and the user, and not on the divergence accumulated over the filtering time constant, τ. This change eliminates the dominant term from the single-frequency ionosphere error expression, (10), and yields

$$\sigma_{iono\_df,i}\left(E_i\right) = OF \cdot \sigma_{vig} \cdot X . \quad (13)$$

Whereas divergence limits smoothing for the single-frequency case, the smoothing time can be significantly increased with dual frequencies. Longer filtering times reduce ground and airborne receiver noise. As suggested by Shively [9], it is reasonable to expect that code noise and multipath might be reduced by a factor of 2 using a longer smoothing time. Based on this assertion, the expression for ground noise in the dual-frequency case is

$$\sigma_{gnd\_df,i}\left(E_i\right) = \sqrt{\frac{1}{4}\left(\frac{\sigma_{RR}}{2}\right)^2 + 0.04^2 + \left(\frac{0.01}{\sin(E_i)}\right)^2} . \quad (14)$$

The reduced dual-frequency airborne noise term is

$$\sigma_{air\_df,i}\left(E_i\right) = \frac{1}{2}\sqrt{\sigma^2_{air\_noise,i} + \sigma^2_{air\_multipath,i}} . \quad (15)$$

Combining these three curves, (13)-(15), and continuing to neglect troposphere error, the total sigma for the dual-frequency case is dramatically lower than that for both the nominal and the reduced airborne noise models, as shown in Figure 2.

BIAS-PROTECTION STRATEGIES

In order to ensure integrity given possible measurement biases, the user VPL must be equal to or larger than the $\mathrm{VPL}_{\mathrm{bias}}$ (4). If the bias and sigma models defined in the previous sections are broadcast to the aircraft, then the exact $\mathrm{VPL}_{\mathrm{bias}}$ expression can be evaluated. Alternatively, if bias parameter terms are not transmitted to the airborne user, then $\mathrm{VPL}_{\mathrm{bias}}$ must be conservatively approximated by inflating the broadcast sigma. This section details these bias-protection strategies, namely bias-parameter transmission and sigma-inflation. Four methods of sigma-inflation are considered here: relative inflation, excess-mass inflation, offline position-domain inflation and real-time position-domain inflation. These sigma-inflation methods achieve progressively sharper bounds at the expense of greater complexity.

Bias-Parameter Transmission

Because bias-parameter transmission implements the exact $\mathrm{VPL}_{\mathrm{bias}}$ expression, (4), it always achieves an availability that is equal to or better than other bias-protection strategies. As a practical detail, implementing bias-parameter transmission requires the definition of a new message type that incorporates one bias parameter, μ_i, for each differential correction. To preserve VHF Data Broadcast (VDB) bandwidth, this new message would most likely be transmitted at a lower update rate than that used for the standard LAAS Type 1 message.

Relative Inflation

The simplest sigma-inflation approach is relative inflation. Like other sigma-inflation methods, relative inflation ensures that the aircraft evaluates a $\mathrm{VPL}_{\mathrm{nom}}$ expression that conservatively approximates $\mathrm{VPL}_{\mathrm{bias}}$. Relative-inflation, previously described by several authors including [4] - [7], makes the assumption that biases are proportional to the sigmas for each ranging source. In this sense, relative inflation implicitly assumes a sigma-relative bias model, which may or may not be a good model for the actual system.

For relative-inflation, the key bounding parameter is, $\tilde{\mu}_{\max}$, a term which describes the worst bias-to-sigma ratio over all satellites, i, as a function of their elevations, E_i.

$$\tilde{\mu}_{\max} = \max_{E_i}\left(\tilde{\mu}_i(E_i)\right), \qquad \tilde{\mu}_i(E_i) = \left|\mu_i(E_i)/\sigma_i(E_i)\right| \quad (16)$$

To provide a formal error bound, the $\tilde{\mu}_{\max}$ parameter should be defined based on a minimum σ_i model that uses the smallest possible user airborne term, σ_{air}, and the shortest possible separation distance for ionosphere and troposphere gradients, $X = 0$. Evaluating $\tilde{\mu}_{\max}$ for this case and substituting into equation (4), for $\mathrm{VPL}_{\mathrm{bias}}$, provides the following conservative approximation.

$$\begin{aligned}\mathrm{VPL}_{\mathrm{bias}} &= K_{ffmd}\sqrt{\sum_{i=1}^{N} S_{v,i}^2\sigma_i^2} + \sum_{i=1}^{N}\left|S_{v,i}\mu_i\right| \\ &\le K_{ffmd}\sqrt{\sum_{i=1}^{N} S_{v,i}^2\sigma_i^2} + \tilde{\mu}_{\max}\cdot\sum_{i=1}^{N}\left|S_{v,i}\sigma_i\right|\end{aligned} \quad (17)$$

Taking advantage of a property of vector norms [12], this inequality may be rewritten more compactly, as $\mathrm{VPL}_{\mathrm{rel}}$.

$$\mathrm{VPL}_{\mathrm{rel}} = \xi_R K_{ffmd}\sqrt{\sum_{i=1}^{N} S_{v,i}^2\sigma_i^2} \ge \mathrm{VPL}_{\mathrm{bias}} \quad (18)$$

In this compact form, the term ξ_R is an inflation factor for the total-error standard deviation, σ_i. The parameter N, which indicates the largest number of satellites in view at any epoch, is set to 12 satellites for this analysis.

$$\xi_R = 1 + \frac{\tilde{\mu}_{\max}\sqrt{N}}{K_{ffmd}} \quad (19)$$

This inflation factor applies to the total sigma for each ranging source; the total sigma, however, consists of four error terms, of which the LAAS ground facility only controls three: the ground, ionosphere and troposphere error contributions. The ground facility has no knowledge of the airborne sigma, $\sigma_{air,i}$, which may vary from aircraft to aircraft, nor any means to alter this term. Hence, in order to achieve the desired total inflation, the broadcast must provide additional margin in the ground sigma in order to establish implicit inflation for $\sigma_{air,i}$. The modified expression for the ground sigma, $\sigma_{gnd\_rel,i}$, should be computed using the maximum possible value of $\sigma_{air,i}$ that any approaching aircraft might use.

$$\sigma_{gnd\_rel,i}^2 = \xi_R^2\sigma_{gnd,i}^2 + \left(\xi_R^2 - 1\right)\sigma_{air,i}^2 \quad (20)$$

Excess-Mass Inflation

Excess-mass inflation is a second sigma-inflation approach. This approach embeds ranging biases in individual broadcast sigma terms in a closed-form manner. Unlike the relative inflation method, the excess-mass inflation technique makes no assumption about the bias model. The excess-mass approach is not unique in this respect, as Shively has proposed another closed-form, model-free method [13], which is not discussed here.

The concept behind the excess-mass bounding technique is to represent biased Probability Distribution Functions (PDFs) as unbiased functions with a total integral greater than one [14]. Figure 3 illustrates a sample excess-mass function bounding a biased-Gaussian distribution. As shown in the figure, the excess-mass bound is not everywhere a tight-bound. For this reason, the excess-mass approach tends to perform poorly if the bias is significantly larger than the sigma for the same satellite.

As the excess-mass concept was originally introduced for the Wide Area Augmentation System (WAAS) [15], further developments are required to adapt the excess-mass concept to LAAS. These derivations of the LAAS excess-mass equations are treated rigorously in the Appendix and summarized in brief in this section. The basic requirement for the excess-mass function is that it be everywhere greater than the modeled error distribution. If the modeled error distribution is a normal distribution with a bias, μ_i, and a standard deviation, σ_i, then a conservative excess-mass function can be defined using two parameters, an inflation, ξ_i and a total mass, k_i.

$$\mathcal{N}(\mu_i,\sigma_i) \le k_i\cdot\mathcal{N}\left(0,\xi_i\sigma_i\right) \quad (21)$$

As shown in the appendix, closed-from expressions for the inflation and mass parameters can be derived to optimize the sharpness of the excess-mass overbound.

$$\begin{aligned}\xi_i &= \tfrac{1}{2}\tilde{\mu}_i + \sqrt{\left(\tfrac{1}{2}\tilde{\mu}_i\right)^2 + 1} \\ k_i &= \xi_i\exp\left(\tfrac{1}{2}\tilde{\mu}_i\xi_i^{-1}\right)\end{aligned} \quad (22)$$

Using this conservative form, an approximate excess-mass protection level, $\mathrm{VPL}_{\mathrm{EM}}$, can be implemented.

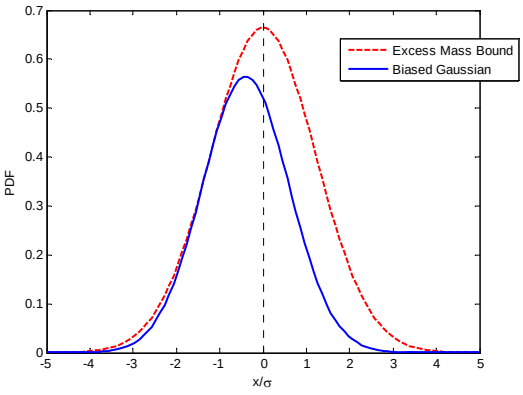

Figure 3. Excess-Mass PDF Bound

$$\mathrm{VPL}_{\mathrm{EM}} = K_{FFMD}\sqrt{\sum_{i=1}^{N} S_{v,i}^2 \xi_{EM,i}^2 \sigma_i^2} \geq \mathrm{VPL}_{\mathrm{bias}} \qquad (23)$$

Here, the total excess-mass inflation, $\xi_{EM,i}$, is derived by combining the mass and inflation parameters, given by (22), as follows.

$$\xi_{EM,i} = \xi_i K_{EM} / K_{FFMD} \qquad (24)$$

$$K_{EM} = \sqrt{2}\,\mathrm{erfc}^{-1}(\mathrm{erfc}\left(K_{FFMD}/\sqrt{2}\right)/\prod_{i=1}^{N} k_i) \qquad (25)$$

In these equations, the modified K-factor parameter, K_{EM}, accounts for the excess-mass parameters, k_i, by decreasing the allowed integrity risk probability. The resulting inflation factor, $\xi_{EM,i}$, is specific to each ranging source, *i*. Since the only satellite-specific sigma parameter broadcast in the VDB message is $\sigma_{gnd\_EM,i}$, this term must be defined carefully to implicitly inflate the $\sigma_{air,i}$ and $\sigma_{iono,i}$ terms, in the manner of (20).

$$\sigma_{gnd\_EM,i}^2 = \xi_{EM}^2 \sigma_{gnd,i}^2 + \left(\xi_{EM}^2 - 1\right)\left(\sigma_{air,i}^2 + \sigma_{iono,i}^2\right) \qquad (26)$$

Offline and Real-Time Position-Domain Inflation

The two previous inflation methods were designed to protect integrity for all satellite geometries. In practice, however, certain pathological worst-case geometries are not observed by airports in the Conterminus United States (CONUS). Consequently, a sharper inflation factor can be derived by taking site-specific geometry information into account. This approach, which requires simulation of the satellite constellations observed by each LAAS facility, is referred to as a position-domain inflation approach. In the position-domain approach, the inflation factor applies directly to the VPL and covers biases for *all* visible satellites, taken together. This position-domain inflation concept is a natural extension of the Position-Domain Monitor (PDM) concept, a proposed modification for LAAS which would validate measurement quality by computing position solutions for all subsets of approved satellites that a user might possibly employ for navigation [16]-[18].

The primary function of position-domain inflation is to determine a scaling factor that, when multiplied by the nominal VPL, ensures integrity for the biased case. In order to ensure integrity, one of two criteria must be met for all satellite combinations a user might employ. The first criterion applies to available geometries, with $\mathrm{VPL}_{\mathrm{bias}}$ less than VAL. To ensure integrity in these cases, the inflated $\mathrm{VPL}_{\mathrm{nom}}$ expression should always equal or exceed $\mathrm{VPL}_{\mathrm{bias}}$. Considering all geometry subsets, $\lambda(t)$, that are available at an epoch, *t*, the inflation factor for available subsets, ξ_{av}, is

$$\xi_{av}(t) = \max_{\lambda(t):\mathrm{VPL}_{\mathrm{bias}}<\mathrm{VAL}} \left(\frac{\mathrm{VPL}_{\mathrm{bias}}\left(\lambda(t)\right)}{\mathrm{VPL}_{\mathrm{nom}}\left(\lambda(t)\right)} \right). \qquad (27)$$

The second criterion applies to unavailable subsets for which $\mathrm{VPL}_{\mathrm{bias}}$ exceeds VAL. For these cases, integrity is ensured as long as the inflated $\mathrm{VPL}_{\mathrm{nom}}$ expression also exceeds VAL. Thus, the inflation factor for unavailable subsets, ξ_{un}, is

$$\xi_{un}(t) = \max_{\lambda(t):\mathrm{VPL}_{\mathrm{bias}}\geq\mathrm{VAL}} \left(\frac{\mathrm{VAL}}{\mathrm{VPL}_{\mathrm{nom}}\left(\lambda(t)\right)} \right). \qquad (28)$$

Inflating by the larger of ξ_{av} and ξ_{un} ensures that no integrity violation can occur. This rule defines the value for the real-time inflation factor, ξ_{RT}:

$$\xi_{RT}(t) = \max\left(\xi_{av}(t), \xi_{un}(t)\right). \qquad (29)$$

Figure 4 graphically illustrates the two criteria used in defining ξ_{RT}. For all values of VPL_{bias} (horizontal axis), the inflated nominal VPL that is evaluated at the aircraft must not fall in the red-shaded zone; points inside this zone represent integrity violations, as they fail one of the two criteria. For a sample geometry case, all satellite subsets are plotted as crosses. Without inflation, many of the crosses fall in the shaded zone that represents an integrity violation. Inflating $\mathrm{VPL}_{\mathrm{nom}}$ by ξ_{RT} ensures integrity by lifting all the data points into the valid region.

To implement real-time position-domain inflation, a distinct value of ξ_{RT} is needed at each epoch. As an alternative, a single offline inflation-factor, ξ_{OL}, could be derived to protect all epochs during the sidereal day.

$$\xi_{OL} = \max_{t}\left(\xi_{RT}(t)\right) \qquad (30)$$

This offline position-domain inflation, ξ_{OL}, is always equal to or greater than the real-time inflation, ξ_{RT}. Consequently, the real-time solution provides a tighter

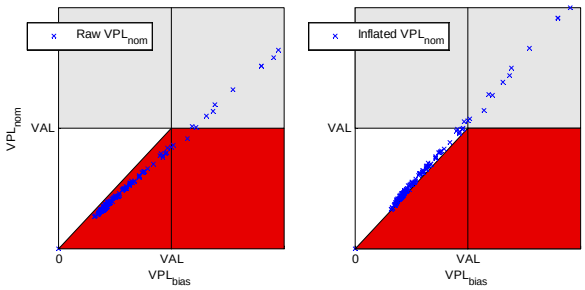

Figure 4. Position-Domain VPL Inflation

overall bound, but at the expense of greater processing requirements for the operational system.

As with other sigma-inflation strategies, the position-domain inflation strategy must also account for limited knowledge of the airborne error bound, $\sigma_{air,i}$. A conservative value of $\sigma_{air,i}$ must be assumed in simulating each geometry subset. Also, because the $\sigma_{air,i}$ term cannot be modified directly by the VDB broadcast, it must be indirectly inflated by applying (20).

AVAILABILITY CALCULATION

The performance of the five bias-protection methods described in the previous section can be assessed by means of an availability simulation. Of the five methods, the bias-bound transmission method will achieve the highest level of availability performance, by definition. The sigma-inflation methods can only approach this limiting availability. Thus, availability simulation can address two relevant issues regarding biased measurements in a CAT III system. First, by simulating the bias-bound transmission strategy, a limit can be established for the largest bias magnitudes that are tolerable for CAT III LAAS. Second, by simulating sigma-inflation strategies, the performance of the bias-bound transmission method can be assessed in comparison to other bias-protection methods which do not require a specification change.

Availability Criterion

System availability is computed as an ensemble average of instantaneous availability for all satellite subsets that occur during a 24-hour day. Satellite subsets are considered at discrete epochs, t_l, spaced at five-minute intervals. For each epoch, satellite geometries are computed with a variable number of unavailable satellites, Q, a parameter which ranges from zero (all satellites available) to a time-varying upper limit (with only four satellites in view). For each value of Q, all possible satellite subset permutations, $\lambda_{m(t_l,Q)}$, are considered.

The availability of each permutation depends on two requirements. First, VPL must be lower than VAL. Second, the geometry must have no more than 2 critical satellites, as required for Cat III operations.

To assess the first requirement, VPL is evaluated separately for each bias-protection strategy. For bias-parameter transmission, the VPL is assessed using (4). For the relative-inflation strategy, VPL is assessed using an inflated nominal VPL, (18). For excess-mass inflation, VPL is assessed using (23). Lastly, in the position-domain inflation cases, VPL is evaluated using (18), with ξ_{OL} or ξ_{RT} substituted for the ξ_R term, as appropriate. In evaluating VPL, the K_{ffmd} factor was set to 6.673, in accordance with the LAAS MASPS [10].

The second availability requirement, which restricts the number of critical satellites, is an extension of the first requirement, which tests VPL. A critical satellite is one which, if suddenly removed from the position solution, would cause VPL to transition to a value greater than VAL. The number of critical satellites can be computed, therefore, by sequentially removing satellites from a subset, one at a time, and comparing VPL to VAL for each reduced satellite set.

For all bias-protection strategies, separate availability simulations were performed for nine different error models. The nine combined error models consisted of combinations of the three bias-bounding models (sigma-relative, absolute, piecewise linear) and the three sigma models (nominal, reduced airborne, and dual-frequency). VAL was set in correspondence with the sigma error model, to ensure adequate availability for the unbiased case. Specifically, VAL was set to 10 m for the nominal sigma, 9 m for the reduced airborne sigma and 5.3 m for the dual-frequency sigma model.

Together the two availability requirements act to screen out poor satellite geometries. As this test is deterministic, the instantaneous availability probability is either 1, if both requirements are satisfied, or 0, if either requirement is lacking.

$$P_{avail,instantaneous}\left(\lambda_{m(t_l,Q)}\right)=\begin{cases}1 & \text{criteria met}\\ 0 & \text{criterion not met}\end{cases} \tag{31}$$

Sensitivity Weights

In computing VPL, the S_v coefficient vector is derived using the standard method for a weighted least-squares solution.

$$S_v=\begin{bmatrix}0 & 0 & 1 & 0\end{bmatrix}\left(G^T\cdot W\cdot G\right)^{-1}G^T\cdot W \tag{32}$$

G is the augmented geometry matrix that consists of unit pointing vectors to each satellite and a column of ones for the unknown clock offset. W is a diagonal matrix with diagonal elements equal to the inverse of the variance for each ranging source.

$$W_{i,j}=\begin{cases}\sigma_i^{-2} & i=j\\ 0 & i\neq j\end{cases} \tag{33}$$

The S_v matrix is not altered when all σ_i values are scaled by the same inflation factor, ξ. For this reason, S_v values were identical for the bias-transmission method and for all sigma-inflation strategies, except excess-mass inflation.

Because the bias-parameter transmission strategy permits changes to the existing LAAS specification, the default weights could be altered to minimize VPL in the presence of biases. A means to implement such a weight optimization for the case of biased measurements was proposed by Blanch [19]. This method was not tested in the present study, since the predicted availability gains are modest and since complexity of the method, based on second-order cone programming, is high.

System Availability Computation

For each bias-protection strategy and for each error model, the total system availability was computed as a weighted average of instantaneous availability for all usable geometry subsets occurring over a 24-hour day. Geometries were simulated for 20 airports in CONUS using a standard "optimized" 24-satellite constellation [20]. In this weighted-average availability, each five-minute interval is weighted uniformly by a factor of 1/*L* (where *L*, the number of time intervals, equals 288). A uniform weight is also assigned to each of the *M* permutations that occur for a particular number of unavailable satellites, *Q*. The probability weight, P_Q, which describes the likelihood of unavailable satellites for the 24-satellite constellation, is based on a set of historical weights, listed in Table 1 [9]. The resulting ensemble average, denoted by angle brackets, predicts availability at a single airport.

$$\left\langle P_{avail} \right\rangle = \sum_{l=1}^{L} \sum_{Q=0}^{N-4} \sum_{m=1}^{M(Q)} \frac{P_Q}{L \cdot M\left(Q\right)} \cdot P_{avail}\left(\lambda_{m(t_l,Q)}\right) \qquad (34)$$

AVAILABILITY COMPARISON

Availability simulations were employed to assess the performance of each of the bias-protection methods. Multiple availability simulations were computed for each airport, to assess the impact of the bias and sigma models. In all, nine error model combinations were considered, including each pairing of the three bias bounds for $\mu_i / \mu_{\max}$ (absolute, relative, and piecewise linear) with each of the three Gaussian σ_i models (nominal, reduced, and dual-frequency). For these nine combinations, the maximum bias level, $\mu_{\max}$, was varied between 2 cm and 80 cm at 2 cm intervals. Thus, with 9 error models and with 40 bias levels, a total of 360 cases were evaluated for each bias-protection method at each airport.

Table 1. Historical Probability Weights

Unavailable Satellites, *Q*, in 24 Satellite Constellation	Standard Probability Weight, P_Q
0	9.85056×10^{-1}
1	1.4839×10^{-2}
2	1.04×10^{-4}
3	1.0×10^{-6}
4+	0

In observing the results of these availability simulations, the most salient feature is the sudden drop in availability that occurs as the bias magnitude $\mu_{\max}$ increases, with all other parameters held constant. Figure 5 clearly illustrates this slope discontinuity. In the figure, the minimum availability over all 20 CONUS airports is plotted as a function of $\mu_{\max}$. The illustrated minimum availability results are based on the nominal model for σ_i (and the corresponding VAL of 10 m). Each of the three biases models, is plotted on a separate chart, proceeding from the absolute model (Figure 5a), to the relative model (Figure 5b), and on to the piecewise linear model (Figure 5c). In each case as $\mu_{\max}$ increases, availability decreases gradually except at one point. This sharp availability jump will be referred to as the transition event, and the largest bias magnitude achieved prior to transition will be referred to as the transition point.

Transition events occur when large biases cause an "all-in-view" geometry to become unavailable. All-in-view geometry combinations are those cases with all satellites operational above a particular airport, either because the constellation is fully functional (Q = 0) or because malfunctioning satellites are on the opposite side of the globe from the simulated airport (Q > 0). The availability after transition is approximated by the availability change upon loss of one all-in-view geometry. The loss of a single all-in-view geometry causes an availability decrease greater than or equal to the weight of the Q = 0 case in the ensemble availability expression (34). This weight, $P_{avail,Q=0}$, is equal

$$P_{avail,Q=0} = \frac{P_Q}{L \cdot M} = \frac{0.985}{288 \cdot 1} = 3.42 \cdot 10^{-3}. \qquad (35)$$

The resulting upper bound on availability after transition is $1 - P_{all-in-view} = 0.9966$. This upper bound can be used to automate the detection of transition points, by searching for the largest value of $\mu_{\max}$ which delivers an availability of at least 0.9966.

For an operational CAT III system, it is important that the all-in-view geometry remain available at all times. Otherwise, there will be times during each sidereal day when the LAAS system is unavailable for navigation. In this sense, the largest tolerable bias equals the transition bias. Any biases larger than the transition bias sacrifices availability for one or more all-in-view geometries (and hence for five or more minutes during the sidereal day).

A principal goal of this paper was to assess the maximum tolerable bias using the best-case bias protection method, that of bias-parameter transmission. Availability simulations indicate that, for the nominal sigma error model and a 10 m VAL, the maximum tolerable bias was only 4 cm – 8 cm. The exact level depends on the bias model used, with the maximum tolerable bias ranging from 4 cm for the absolute model, to 6 cm for the piecewise linear model, and to 8 cm for the sigma-relative model. These low tolerable bias levels represent a significant challenge for the design of CAT III hardware. Preferably, the tolerable bias would be at least 10 cm, or more.

It is significant to note that the worst-case CONUS airports determine the maximum tolerable bias level. When examining the median availability over all CONUS airport, tolerable biases were significantly higher: 42 cm for the absolute model, 74 cm for the piecewise model, and over 80 cm for the sigma-relative model. Median availability plots for the nominal sigma error distribution are shown in Figure 6. Clearly, the biased measurements would not be a problem at most CONUS airports, other than a few worst-case locations.

Similar results are observed for the two other sigma models (reduced airborne and dual-frequency). For the reduced airborne noise model with a 9 m VAL, the tolerable bias level was 4 cm – 8 cm for the worst-case airport and 42 – 78 cm for the median airport. For the dual-frequency error model with a 5.3 m VAL, tolerable bias levels were 14 – 22 cm for the worst-case airport and 34-70 cm for the median airport. Surprisingly, the dual-frequency error model tolerates larger biases than the nominal model, even with the tighter 5.3 m VAL.

This result reflects extra availability margin in the dual-frequency case. That is, the VAL for the nominal (10 m) and reduced airborne (9 m) models was set to ensure availability of at least 0.9999 in the unbiased case. In the dual-frequency case, VAL was set to its specified value of 5.3 m, and the resulting baseline availability, with no biases, was even higher than 0.9999.

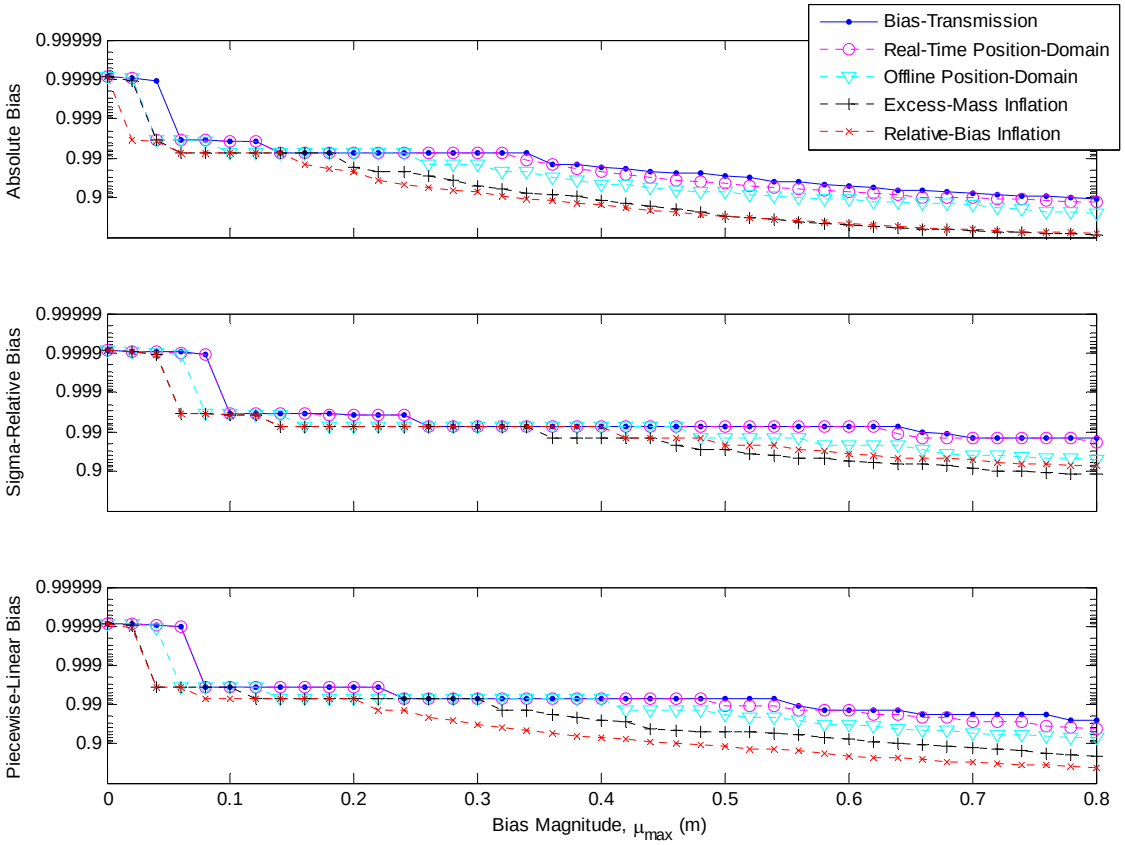

Figure 5. Minimum Airport Availability with Three Bias Models (and Nominal σ Model, VAL = 10 m)

The second principal goal of the availability simulations was to compare performance of sigma inflation to that of bias-parameter transmission. The relative performance ranking was generally consistent among all sigma inflation strategies. Real-time position-domain inflation always performed better than offline position-domain inflation. The position-domain inflation techniques always outperformed relative inflation and excess-mass inflation. The performance of these latter methods, however, depended on the bias model. The relative inflation technique always outperformed excess-mass inflation for the sigma-relative bias model, to which relative inflation is tuned. The excess-mass approach always outperformed the relative inflation approach for both the piecewise-linear and absolute bias models, with one exception (which occurred for the dual-frequency sigma model in the median-availability case).

Transition points for all models are tabulated in Table 2 and Table 3. The former table lists transition points for the minimum-availability airport, and the latter, for the median-availability airport.

Based on these tables, it can be concluded that the tolerable biases for the closed-form sigma inflation techniques (relative and excess-mass inflation) were generally half the tolerable biases for bias-parameter transmission. For this reason, the closed-form sigma inflation techniques are not recommended for application at the minimum-availability CONUS airports. By comparison, the closed-form sigma inflation methods provided very reasonable bias tolerance at the median availability CONUS airport, in the 16 – 46 cm range depending on the sigma error model.

The real-time position-domain inflation technique performs very well even at worst-case CONUS airports. In fact, the tolerable biases for this position-domain technique nearly match the upper limits established for bias-parameter transmission.

The major disadvantage of the real-time position-domain inflation method (and of all sigma-inflation methods) is sensitivity to unknown variations in the σ_{air} parameter. Significant availability may be lost for the position-domain inflation method if the σ_{air} parameter value must

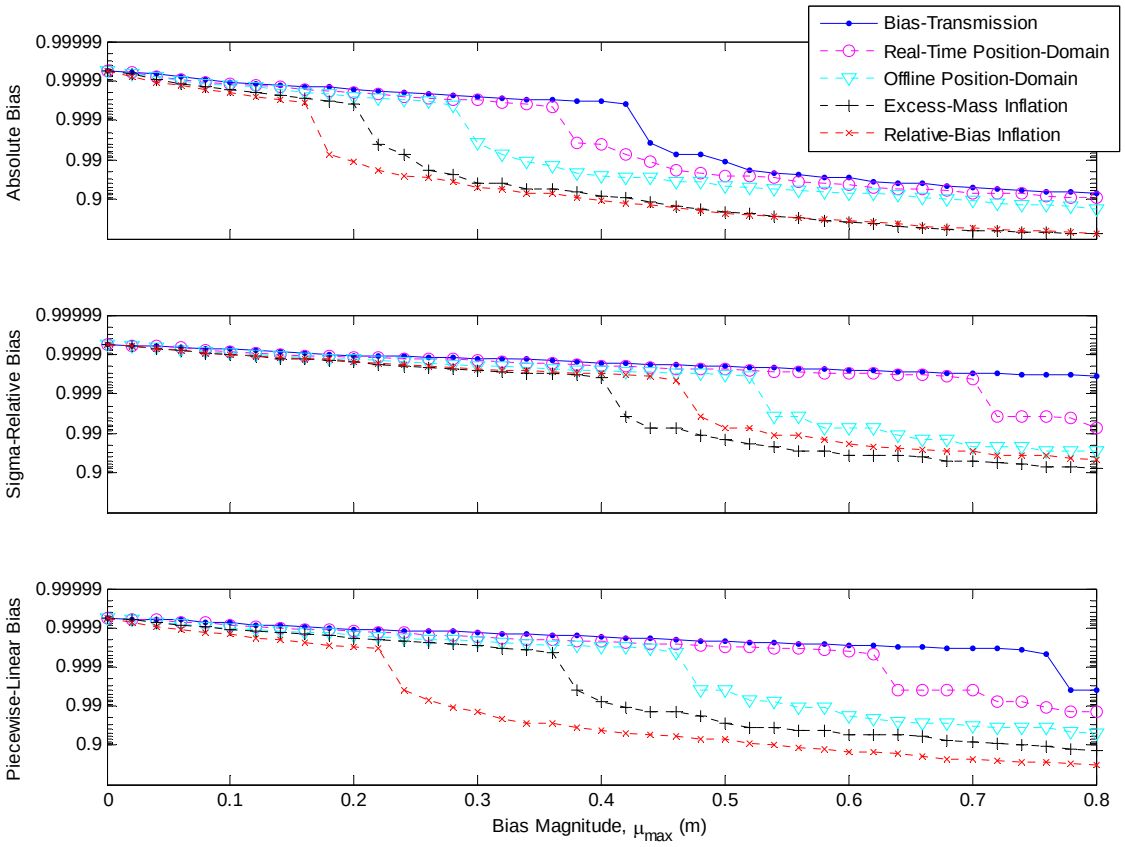

Figure 6. Median Airport Availability with Three Bias Models (and Nominal σ Model, VAL = 10 m)

be estimated conservatively. As an example, consider an airport with two sets of approaching aircraft, one set using the nominal sigma model and a second set using the reduced airborne sigma model. For a sigma-inflation technique to protect both cases, the more conservative must be used in the definition of the inflation factor. Performance suffers accordingly. By contrast, in bias-parameter transmission, the exact VPL expression is evaluated at the aircraft, which has full knowledge of its own σ_{air}. Thus the bias-parameter transmission approach need not compensate to cover the worst of the two σ_{air} parameters.

Figure 7 illustrates this hypothetical case by comparing the performance of real-time position-domain inflation to that of bias-parameter transmission. A 10 m VAL is assumed for both sets of approaching aircraft. For aircraft with the higher σ_{air} parameter, based on the nominal model, the tolerable bias is 4 – 8 cm for bias transmission (at the worst availability airport). For aircraft with the reduced σ_{air} parameter, the maximum tolerable bias increases dramatically, up to the range of 16 – 38 cm. This improvement applies only to for bias-parameter transmission. By comparison, the performance of the position-domain inflation method is always the same, regardless of the aircraft error model. The tolerable bias with this sigma-inflation method is only 2 – 8 cm, on par with bias-transmission for the nominal σ_{air} case, but substantially inferior to bias-transmission for the reduced σ_{air} case. Based on this analysis, it may be concluded that bias-parameter transmission is preferable to sigma-inflation if σ_{air} varies significantly among approaching aircraft. Otherwise, bias-parameter transmission offers little performance advantage over the best-performing sigma inflation methods, which would require no changes to the existing LAAS specification.

SUMMARY

Given the possibility of measurement biases, LAAS integrity requirements motivate the definition of a conservative protection level equation that incorporates a bias bound parameter for each ranging source. The major challenge of implementing this modified protection level at the airborne receiver involves the specification changes

Table 2. Largest Bias that achieves a *Minimum* Availability of 0.999

	Dual Frequency Sigma			Reduced Airborne Sigma			Nominal Sigma		
	Absolute Bias	**Relative Bias**	**Piecewise Bias**	**Absolute Bias**	**Relative Bias**	**Piecewise Bias**	**Absolute Bias**	**Relative Bias**	**Piecewise Bias**
Transmit Bias	0.14	0.30	0.22	0.04	0.08	0.08	0.04	0.08	0.06
Real-Time Position Domain	0.12	0.28	0.20	0.04	0.08	0.08	0.02	0.08	0.06
Offline Position Domain	0.10	0.20	0.16	0.02	0.06	0.06	0.02	0.06	0.04
Excess-Mass Inflation	0.06	0.14	0.10	0.02	0.04	0.04	0.02	0.04	0.02
Relative-Bias Inflation	0.06	0.16	0.08	0.02	0.04	0.02	0.00	0.04	0.02

Table 3. Largest Bias that achieves a *Median* Availability of 0.999

	Dual Frequency Sigma			Reduced Airborne Sigma			Nominal Sigma		
	Absolute Bias	**Relative Bias**	**Piecewise Bias**	**Absolute Bias**	**Relative Bias**	**Piecewise Bias**	**Absolute Bias**	**Relative Bias**	**Piecewise Bias**
Transmit Bias	0.34	0.70	0.58	0.42	0.78	0.72	0.42	0.8+	0.76
Real-Time Position Domain	0.30	0.62	0.52	0.36	0.66	0.64	0.36	0.70	0.62
Offline Position Domain	0.24	0.46	0.38	0.28	0.48	0.48	0.28	0.52	0.46
Excess-Mass Inflation	0.14	0.32	0.26	0.20	0.32	0.32	0.20	0.40	0.36
Relative-Bias Inflation	0.16	0.38	0.18	0.14	0.40	0.24	0.16	0.46	0.22

that would be required to transmit bias parameters to the airborne user. As an alternative to this bias-parameter transmission strategy, sigma-inflation techniques can be defined that conservatively approximate the desired protection level equation without requiring any specification change. Although bias-parameter transmission will always outperform sigma-inflation, the sigma-inflation methods are generally preferable to maintain compliance with existing specifications.

The maximum tolerable bias for CAT III LAAS was determined by computing availability simulations for the bias-parameter transmission method. Availability simulations indicate that, for the nominal LAAS error model and a 10 m VAL, the maximum tolerable bias at the worst-case CONUS airport is only 4 – 8 cm. Constructing a system that achieves this bias bound represents a significant challenge for CAT III LAAS, assuming that the fielded hardware performs at the level of the nominal LAAS error curves.

The tolerable bias improves dramatically if dual frequency signals are available. With dual-frequencies and a 5.3 m VAL, the maximum tolerable bias rises to a level of 14 – 30 m, with the specific level depending on the bias model used in simulation. Achieving this level of tolerable bias should be fully feasible for CAT III LAAS.

Availability simulations indicated the potential for sigma-inflation methods to perform nearly as well as bias-parameter transmission methods. Although closed-form sigma inflation techniques tolerated only half the maximum biases achieved by bias transmission, a real-time position-domain inflation technique performed nearly on par with bias-parameter transmission.

The only significant disadvantage of sigma-inflation arises when approaching aircraft use differing models for airborne receiver noise, in which case the bias-transmission method may substantially outperform sigma inflation. With this case excepted, the marginal performance gains for bias-transmission over sigma-inflation do not justify any changes to the existing LAAS specifications to aid in protection of integrity for the biased measurement case.

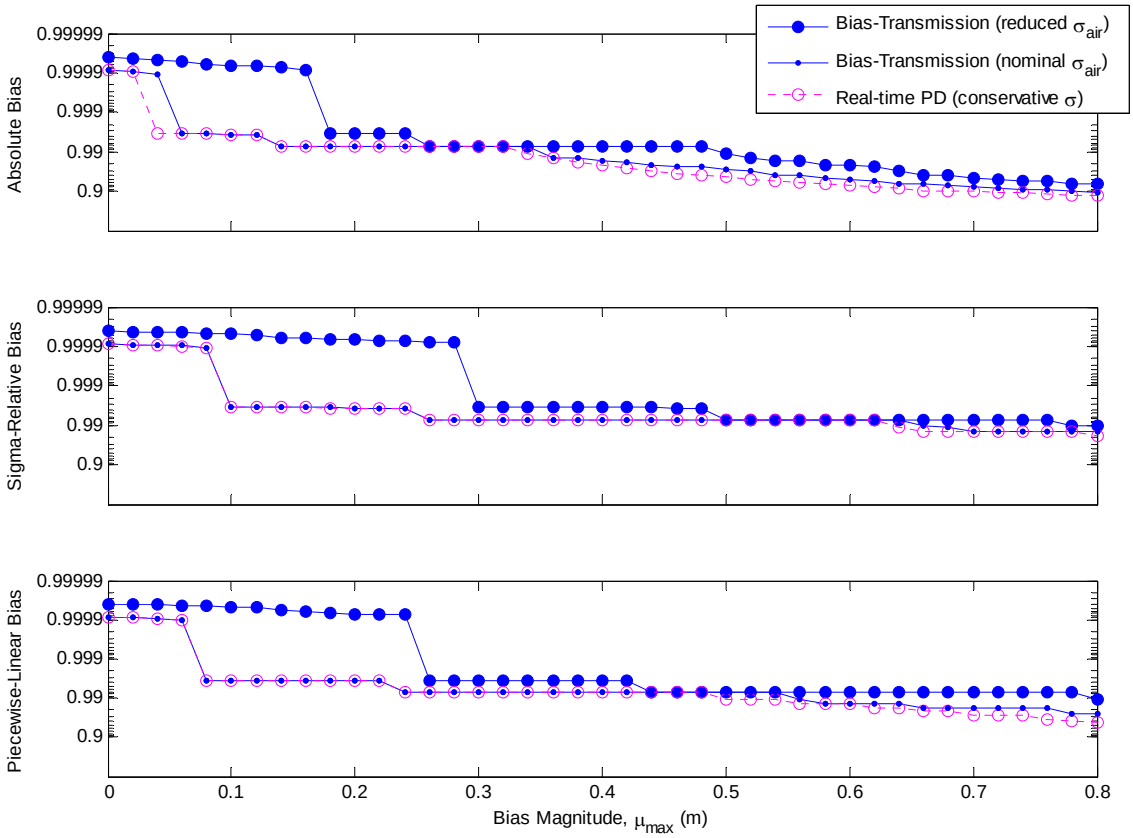

Figure 7. Median Airport Availability with Three Bias Models (VAL = 10 m): Case of aircraft approaching with one of two error models for σ_{air} (nominal or reduced)

ACKNOWLEDGEMENTS

The authors gratefully acknowledge the Federal Aviation Administration Satellite Navigation LAAS Program Office (AND-710) for supporting this research. The opinions discussed here are those of the authors and do not necessarily represent those of the FAA or other affiliated agencies.

REFERENCES

[1] J. Rife, S. Pullen, B. Pervan, and P. Enge, *Paired Overbounding and Application to GPS Augmentation*, Proceedings of IEEE Positioning, Navigation and Location Symposium, 2004, pp. 439 - 446.

[2] RTCA Inc, *GNSS-Based Precision Approach Local Area Augmentation System (LAAS) Signal-in-Space Interface Control Document (ICD)*, RTCA/DO-246B, November 28, 2001.

[3] RTCA Inc, *Minimum Operational Performance Standards for GPS Local Area Airborne Equipment*, RTCA/DO-253A, November 28, 2001.

[4] B. DeCleene, *Defining Pseudorange Integrity – Overbounding*, Proceedings of ION GPS 2000, pp. 1916 - 1924.

[5] F. van Graas, V. Krishnan, R. Suddapalli, T. Skidmore, Conspiring Biases in the Local Area Augmentation System, Proceedings of ION Annual Meeting 2004, pp. 300-307.

[6] C. Shively, *A Proposed Method for Including the Mean in the LAAS Correction Error Bound by Inflating the Broadcast Sigma*, MITRE/CAASD Memorandum, 2000.

[7] B. Pervan, S. Pullen, and I. Sayim, *Sigma Estimation, Inflation, and Monitoring in the LAAS Ground System*, Proceedings of ION GPS 2000, pp. 1234 - 1244.

[8] G. McGraw, T. Murphy, M. Brenner, S. Pullen and A.J. Van Dierendonck, *Development of LAAS Accuracy Models*, Proceedings of ION GPS 2000, pp. 1212 - 1223.

[9] C. Shively and T. Hsiao (2004). *Availability Enhancements for Cat IIIb LAAS*, NAVIGATION, Journal of the Institute of Navigation, v. 51, n. 1, 2004, pp. 45 – 57.

[10] RTCA Inc, *Minimum Aviation System Performance Standards for the Local Area Augmentation System (LAAS)*. RTCA/DO-245, 1998.

[11] P. Hwang, G. McGraw, J. Bader, *Enhanced Differential GPS Carrier-Smoothed Code Processing Using Dual-Frequency Measurements*, NAVIGATION, Journal of the Institute of Navigation, v. 46, n. 2, 1999, pp. 127 – 137.

[12] G. Golub and C. Van Loan, *Matrix Computation*, Johns Hopkins University Press, 1996, pp. 52 – 53.

[13] C. Shively, *A Proposed Method for Including the Mean in the LAAS Correction Error Bound by Inflating the Broadcast Sigma*, MITRE/CAASD Memorandum, 2000.

[14] J. Rife, T. Walter, and J. Blanch, *Overbounding SBAS and GBAS Error Distributions with Excess-Mass Functions*, Proceedings of the International Symposium on GNSS/GPS, Sydney, Australia, 2004.

[15] T. Walter, J. Blanch, and J. Rife, *Treatment of Biased Error Distributions in SBAS*, Proceedings of the International Symposium on GNSS/GPS, Sydney, Australia, 2004.

[16] K. Markin and C. Shively, *A Position-Domain Method for Ensuring Integrity of Local Area Differential GPS (LDGPS)*, Proceedings of ION Annual Meeting 1995, pp. 369-380.

[17] R. Braff, *Position Domain Monitor (PDM) Performance Analysis for CAT III*, MITRE/CAASD Memorandum, 2002.

[18] J. Lee, *LAAS Position Domain Monitor Analysis and Test Results for CAT II/III Operations*, Proceedings of ION GPS 2004, pp. 2786 - 2796.

[19] J. Blanch, T. Walter, and P. Enge, *Error Bound Optimization Using Second Order Cone Programming*, Proceedings of ION National Technical Meeting, 2005, pp. 1009 - 1013.

[20] RTCA Inc, *Minimum Operational Performance Standards for GPS WAAS Airborne Equipment*, RTCA/DO-229A, June 8, 1998.

APPENDIX

When defining an excess-mass bound for a Gaussian distribution with a nonzero mean, two parameters must be selected for each ranging source: ξ_i and k_i. The ξ_i parameter scales the width of the excess-mass function, $f_{EM,i}$, and the k_i parameter scales its height. If the excess-mass function is a normal distribution, $\mathcal{N}$, for instance, it has the following form.

$$f_{EM,i} = k_i \cdot \mathcal{N}\left(0, \xi_i \sigma_i\right) \tag{36}$$

As discussed in [14], a set of excess-mass functions can be substituted for biased error distributions in computing

a position-domain error bound. The position-domain bounding function, $f_{EM,pos}$, has the following form.

$$f_{EM,pos} = \left(\prod_{i=1}^{N} k_i \right) \cdot \mathcal{N}\left(0, \sqrt{\sum_{i=1}^{N} S_{v,i}^2 \xi_i^2 \sigma_i^2} \right) \tag{37}$$

The VPL derived from this bounding function has the conventional form.

$$VPL_{H0,EM} = K_{EM} \sqrt{\sum_{i=1}^{N} S_{v,i}^2 \xi_i^2 \sigma_i^2} \tag{38}$$

The excess-mass VPL differs from the conventional VPL in its sigma-inflation and in the definition of the K-factor, which is modified to account for a reduction in the probability allotment for hazardously misleading information. For example, the effective Fault-Free Missed Detection (FFMD) probability for the excess-mass method is

$$P_{EM} = \left(\prod_{i=1}^{N} k_i \right)^{-1} P_{FFMD} . \tag{39}$$

The corresponding K_{EM} term can be computed from K_{FFMD} according to (25), given that the excess-mass function has a Gaussian form.

$$K_{EM} = \sqrt{2}\, \mathrm{erfc}^{-1}(\mathrm{erfc}\left(K_{FFMD} / \sqrt{2} \right) / \prod_{i=1}^{N} k_i) \tag{25}$$

For the purpose of availability maximization, the optimal values for the ξ_i and k_i parameters are those that result in the lowest $VPL_{H0,EM}$. This optimization is expensive to compute, since the S_v vector changes for each geometry subset at each epoch for all airports. As an alternative method to ensure high availability with reduced computation effort, the parameters may be selected based on a tight-fit criterion.

For a tight fit, the excess-mass bound should be tangent to the underlying biased Gaussian distribution at exactly one point. This tangency condition places the following constraint relationship on ξ_i and k_i, as a function of the normalized bias parameter, $\tilde{\mu}_i$.

$$k_i = \xi_i \exp\left(\frac{\tilde{\mu}_i^2}{2\left(\xi_i^2 - 1 \right)} \right) \tag{40}$$

A tight fit should also minimize the difference between the overbounding excess-mass function and the nominal biased-Gaussian distribution. A convenient metric to describe this difference is the functional one-norm. If the difference between the two normal distributions is

$$\Psi = k_i \cdot \mathcal{N}\left(0, \xi_i \sigma_i \right) - \mathcal{N}(-\mu_i, \sigma_i) , \tag{41}$$

then the functional one-norm can be defined as follows.

$$\begin{aligned} \left\| \Psi \right\|_1 &= 2 \int_{-\infty}^{0} \left| k_i \cdot \mathcal{N}\left(0, \xi_i \sigma_i \right) - \mathcal{N}(-\mu_i, \sigma_i) \right| dx \\ &= k_i - \mathrm{erfc}\left(-\tfrac{1}{\sqrt{2}} \tilde{\mu}_i \right) \end{aligned} \tag{42}$$

This norm is treated as symmetric across zero, so it is computed along the negative axis and then doubled. The symmetry across zero implies that the appropriate tight fit condition along the positive axis uses a bias of $+\mu_i$ rather than $-\mu_i$. Substituting (40) into (42) and minimizing gives the following result.

$$\xi_i = \tfrac{1}{2} \tilde{\mu}_i + \sqrt{\left(\tfrac{1}{2} \tilde{\mu}_i \right)^2 + 1} \tag{43}$$

This result can be derived by taking the first derivative of (42) with respect to ξ_i, and setting the result to zero to find the minimum of the one-norm.

$$\frac{\partial}{\partial \xi_i} \left\| \Psi \right\|_1 = \exp\left(\frac{\tilde{\mu}_i^2}{2\left(\xi_i^2 - 1 \right)} \right) \left(1 - \frac{\xi_i^2 \tilde{\mu}_i^2}{\left(\xi_i^2 - 1 \right)^2} \right) = 0 \tag{44}$$

The exponential expression can be shown to be always positive, so the right hand term, in parentheses can be set equal to zero and solved to give (43). Inserting (43) into (40) gives an expression for k_i.

$$k_i = \xi_i \exp\left(\tfrac{1}{2} \tilde{\mu}_i \xi_i^{-1} \right) \tag{45}$$

The resulting expressions for the two excess-mass parameters, ξ_i and k_i, were given as (22) in the body of this paper. Though not designed specifically to minimize the $VPL_{H0,EM}$ equation, these parameter choices still provide a tight bound that results, correspondingly, in an availability computation that is nearly optimal.